

Spatial-temporal Variation and Health Risk Assessment of Fluoride in Surface Water in the Tibetan Plateau

yi yang (✉ yangyi.19b@igsnr.ac.cn)

Institute of Geographic Sciences and Natural Resources Research Chinese Academy of Sciences

Ru Zhang

Institute of Geographic Sciences and Natural Resources Research Chinese Academy of Sciences

Fengying Zhang

China National Environmental Monitoring Center

Yonghua Li

Institute of Geographic Sciences and Natural Resources Research Chinese Academy of Sciences

Research Article

Keywords: Fluoride, Surface water, Tibetan Plateau, Health risk assessment, Climate change

Posted Date: January 20th, 2022

DOI: <https://doi.org/10.21203/rs.3.rs-1252090/v1>

License:   This work is licensed under a Creative Commons Attribution 4.0 International License.

[Read Full License](#)

Abstract

The Tibetan Plateau (TP) is known as the “Asian Water Tower” and provides vital drinking water for residents of China and Southeast Asian countries. However, large-scale regional research on water quality in this climate-sensitive and eco-fragile area is still lacking. Considering that drinking from fluoride-contaminated water has posed serious health concerns worldwide, especially in Asian countries, it is urgent to clarify the spatial-temporal distribution characteristics, influencing factors, and health risk of fluoride in surface water in the TP. In this study, a total of 2697 surface water samples from major rivers and typical lakes in the TP were systematically analysed. Overall, fluoride concentrations ranged from 0.005 mg L⁻¹ to 6.240 mg L⁻¹ and varied among water periods, water basins and even water types. Pearson’s correlation analysis showed that the distribution of fluoride concentration was closely related to regional climate and positively correlated with anthropogenic activities. Probabilistic health risk assessment revealed that potential hazards in the Inner basin remained highest for all age groups (HR>1), especially for infants and adults (HR>3), while the risks in most other water basins were acceptable (HR < 1). In addition, more than 75% of the residents affected by the surface water in the TP were assessed as having a low fluoride exposure health risk. Our findings can provide scientific support for fluorosis prevention, as well as guide water resource utilization in the TP and adjacent region.

1. Introduction

Fluoride is widely distributed in the natural environment and closely affects human health (Liu et al., 2021). In general, 80–90% of the fluoride in the human body is concentrated in the bones and teeth. Appropriate absorption of fluoride is beneficial to human growth and bone metabolism (Meng et al., 2021). However, excessive fluoride intake leads to dental fluorosis, skeletal fluorosis and other diseases, which seriously affects health (Yin et al., 2021). Numerous studies have shown that high fluoride concentrations in drinking water (> 1.0 mg L⁻¹) can cause dental fluorosis and even bone fluorosis (Ahada et al., 2019; Narsimha et al., 2018).

Drinking water with a high fluoride concentration remains a challenge impacting the health of millions of people worldwide (Marghade et al., 2020; Narsimha et al., 2018). Drinking water fluorosis occurs widely worldwide and is prevalent to varying degrees in more than 50 countries and regions in Asia (India, Bangladesh, China, Thailand, Sri Lanka, etc.), Europe (Russia, Bulgaria, Italy, etc.), Africa, the Americas and Oceania (Zhang et al., 2016). China used to have one of the most serious epidemics of drinking-type fluorosis, with 1115 counties, 75,287 villages, and 72.07 million people affected (Zhang et al., 2020).

The Tibetan Plateau (TP) is one of the areas where both brick tea-type fluorosis and drinking-type fluorosis are prevalent (Lou et al., 2020). Researchers considered drinking brick tea to be the main cause of fluorosis in the TP because the average fluoride content of brick tea in this area is approximately 800 mg kg⁻¹, which is far above the national safe threshold of brick tea fluoride concentration (300 mg kg⁻¹) (Zhang et al., 2019; GB 19965, 2005). Therefore, previous studies on fluorosis in the TP were mainly focused on brick tea, ignoring the endemic of drinking-type fluorosis, which may mislead fluorosis

prevention and treatment in the TP. In addition, it has been confirmed that compared with other fluorosis endemic areas, the same quantity of brick tea fluoride intake in the TP causes more severe fluorosis symptoms (Liu et al., 2020), which suggests that the superposition of fluoride intake via other pathways, such as through drinking water, makes fluorosis more serious. Unfortunately, to date, no data on the water fluoride concentration in the TP are available in the published literature.

The TP is the cradle of major Chinese river systems, including the Yellow River, Yangtze River, and Mekong River. Moreover, several important rivers in Southeast Asia, such as the Ganges, Indus, and Salween rivers, originate in this region. The TP is considered the “Asian Water Tower”, providing fresh water for nearly one-third of the world’s population (Qiao et al., 2021) and playing a vital role in maintaining human health and economic and social development. The water quality of the TP has a profound influence not only on China but also on all of southeast Asia. Therefore, it is of great significance to study the distribution and influencing factors of water fluoride in the TP.

Currently, the distribution of surface water fluoride is thought to relate to both natural and anthropological factors. Hydrochemical characteristics influenced by regional climate, topography and anthropogenic activities (Yin et al., 2021; Zhang et al., 2019; Liu et al., 2020; Ma et al., 2021). The temporal and spatial distribution of water resources and changes in water quality caused by climate conditions have generated a lot of research interest from scientists and governments in various countries (Zhang et al., 2021). However, most studies have focused on the impact of climate change on the amount of water, and relatively few studies have concentrated on changes in water quality (Ran et al., 2021; Duan et al., 2020). There is almost no discussion on the impact of climate change on fluoride distribution in water. Climate change affects the regional surface water cycle by changing the temporal and spatial distribution of meteorological factors such as air temperature and precipitation, influencing the migration and transformation of compounds and ions in the water (Gomiero et al. 2014; Rocha et al., 2015). Moreover, the change in topography in the plateau region leads to an uneven distribution of surface elements and makes the region prone to endemic diseases (Xu et al., 2018; Hettithanthri et al., 2021). Anthropogenic activities, such as effluent discharge, agriculture, will also influence hydrochemical characteristics (Kulk et al., 2021; Markogianni et al., 2016).

In this study, the fluoride concentrations in the surface water of major rivers and typical lakes in the TP were systematically analysed to clarify the spatial-temporal variation in fluoride and to estimate the health risks posed by surface water. Simultaneously, the possible anthropological activities, regional climate, and topography factors affecting the concentration and distribution of fluoride in the TP were discussed. This study is the first attempt to investigate the distribution characteristics, influencing factors, and human health risks of fluoride in the surface water over the TP, and it can provide a scientific basis for fluorosis prevention, water resource utilization, agricultural production, and animal husbandry in the plateau region.

2. Materials And Methods

2.1. Study area

The study area includes the Qinghai Province and the Tibet Autonomous Region (78°23'24"–103°4'12" E; 26°51'–39°12'36" N) comprising the main area of the TP (60.6%). It covers an area of 1.9507 million square kilometres and 118 counties with a total population of 9.43 million (Fig. 1). The TP is the highest of “the three steps of China's terrain”, with an average elevation of 4400 m (Wang et al., 2017). Several famous rivers originate here, including the Yangtze, Yellow River, Brahmaputra, Salween, and Indus rivers. The area also has a high density of lakes, and the lakes in the TP account for 57% of the total lake area and 69% of the inland lake area in China (Pi et al., 2020; Lu et al., 2020). The annual average air temperature of the TP ranges from –6°C in the northwest to 20°C in the southeast (Dong et al., 2020). The annual precipitation is uneven, decreasing from the southwest (2000 mm) to the northwest (less than 50 mm) (Wu et al., 2019).

The main sources of surface water in the TP are precipitation and melting water, with a small interannual variation in river flow (Nury et al., 2021; Wang et al., 2020). In general, the annual flow is mainly concentrated in June to October (rich period), accounting for 75–80% of the annual main flow, and the dry period ranges from December to April, while the remaining months represent flat periods (Liu et al., 2021). It is worth mentioning that water periods in this study were determined by actual measurements in each month, and the specific time of the three periods may slightly change according to different natural factors, such as temperature, precipitation or vegetation cover (Xu et al., 2021).

2.2. Data sources

2.2.1. Water quality data

Water quality data in this study were derived from the China National Eco-environmental Monitoring Network (<http://www.cnemc.cn/>). The dataset contained 2697 monthly samples from 69 monitoring (61 river sampling sites and 8 lake sampling sites) throughout the TP, covering a full 5-year (2016–2020) period.

2.2.2. Watershed landscape and meteorological data

To obtain the water basin dataset over the TP, we used the dataset of river basin maps over the TP from the National Tibetan Plateau Data Center (TPDC) (Zhang et al., 2019). The study area was divided into 10 water basins according to the river network (Brahmaputra, Ganges, Hexi, Indus, Inner, Mekong, Qaidam, Salween, Yangtze and Yellow River) and elevation (Fig. 2, Fig. 3). Elevation were obtained from the Resource and Environment Science and Data Center (<https://www.resdc.cn/>). Slope data were transformed from elevation by using the ArcGIS Surface Toolset.

Local meteorological data of the TP were obtained from the Chinese Meteorological Forcing Dataset provided by the TPDC (Yang et al., 2019). The dataset has a high spatial resolution of 0.1°, with gridded near-surface meteorological data developed specifically for studies of land-surface processes across the TP. The dataset contains air temperature (°C) and precipitation (mm d⁻¹) data.

2.2.3. Night light index

In this study, the analysis data of the night light index come from the visible light imaging linear scanning system of the U.S. National Polar Orbiting Satellite Visible Infrared Imaging Radiometer (VIIRS) (<https://earthdata.nasa.gov/>). The spatial resolution of the VIIRS is 0.75 km, and the spatial resolution of the night lighting products is 0.5 km.

2.3. Statistical analysis

ArcGIS 10.4 software was used to present the spatial distribution of the surface water fluoride concentration. Statistical analysis was conducted in SPSS software (IBM SPSS Statistics 26), and the Pearson's rank correlation coefficient was constructed to analyse the relationship between fluoride and influencing factors. In addition, the human health risk of surface water fluoride in the study area was assessed based on the health risk assessment model recommended by the United States Environmental Protection Agency (USEPA) (USEPA, 1989), and the sensitivity analysis was applied with the Monte Carlo method using the Crystal Ball software (Oracle Crystal Ball version 11.1.2.3).

2.4. Human risk assessment

In this study, the potential human health risk of fluoride was assessed for different age groups due to different behavioural and physiological attributes (USEPA, 2008). According to the differences in environmental exposure behaviour among different age groups, we divided the potentially affected population into four groups: infants (0–3 years old), young children (4–6 years old), children (7–12 years old), teenagers (13–18 years old) and adults (>18 years). Fluoride in water acts as a toxic but noncarcinogenic substance (Yuan et al., 2020). The risk assessment of a toxic substance is generally based on the reference dose (Li et al., 2020).

Fluoride in water enters the human body through ingestion, dermal absorption and inhalation. However, inhalation is not included in this study. Some toxicological data, such as the inhalation reference dose for fluoride and the transfer efficiency from water to air, are unavailable in the database and published literature. Considering the two other exposure pathways, we estimated the daily exposure dose of fluoride through water ingestion and dermal absorption. The formulas for calculating the average daily exposure doses I_i and I_d are as follows, and the values of the parameters are shown in Table 1 (Duan, 2012).

$$I_i = \frac{C \times IR \times EF \times ED}{BW \times AT}$$

1

$$I_d = \frac{C \times SA \times K_p \times F \times ETs \times EF \times ED \times 10^{-3}}{BW \times AT}$$

2

where I_i represents the estimated average daily exposure dose of fluoride through ingestion ($\text{mg kg}^{-1} \text{d}^{-1}$);

I_d represents the estimated average daily exposure dose of fluoride through dermal absorption ($\text{mg kg}^{-1} \text{d}^{-1}$);

C is the measured concentration of fluoride in groundwater (mg L^{-1});

IR is the drinking rate (L d^{-1});

EF is the exposure frequency (d a^{-1});

ED is the exposure duration (a);

BW is the average weights (kg).

AT is the life expectancies of residents (d);

SA is the average skin surface area (cm^2);

K_p is the dermal permeability constant: $10^{-3} \text{ (cm h}^{-1}\text{)}$;

F is the fraction of surface skin contact with water: 0.4 (unit-less);

ETs is the exposure time in the shower (h day^{-1}); and

10^{-3} is the number of L per cm^{-3} .

The noncarcinogen risk assessment model was used in the present study as follows:

$$HR = \frac{\sum I}{D_{Rf}}$$

3

where HR is the noncarcinogenic risk index and D_{Rf} represents the reference dose of a noncarcinogenic substance ($\text{mg kg}^{-1} \text{d}^{-1}$). The fluoride reference dose for human health risk by exposure through consumption of potable water is $0.06 \text{ mg kg}^{-1} \text{d}^{-1}$.

The USEPA health risk assessment guidelines indicate that the threshold of noncarcinogenic risk HR is 1 (Li et al., 2020). An HR value < 1 indicates that the health risk posed by noncarcinogenic substances is within an acceptable level, whereas an HR > 1 indicates that the noncarcinogenic health risk is unacceptable.

All data sources in this study shown in Supplementary Table 1.

Table 1 Human exposure parameters of fluoride

Parameters	Infants (0-3)	Young Children (4-6)	Children (7-12)	Teenagers (12-18)	Adults (>18)
IR	0.49	0.78	1.09	1.59	2.71
EF	365	365	365	365	365
ED	1.5	5.0	9.5	15.0	52.0
BW	9.21	16.65	28.15	47.3	58.55
AT	548	1825	3468	5475	18980
SA	0.45	0.72	1.04	1.47	1.60
ETs	0.069	0.078	0.100	0.120	0.083

3. Results And Discussion

3.1. Spatial-temporal variation in surface water fluoride in the Tibetan Plateau

The overall statistical characteristics of fluoride in surface water in the TP are shown in Table 2. In total, 2697 monthly water fluoride data points at 69 sites were analysed. From 2016 to 2020, the average fluoride concentration showed a downwards trend, decreasing from 0.408 mg L⁻¹ to 0.278 mg L⁻¹. In general, the median concentration was approximately 0.23 mg L⁻¹, and the standard deviation was approximately 0.68. The concentration varied greatly among sampling sites. The maximum concentration exceeded 4.0 mg L⁻¹ each year, while the minimum value stayed at approximately 0.005 mg L⁻¹.

Table 3 is a statistical summary of the fluoride content of surface water in the TP among the dry, flat and rich periods. The fluoride concentration during the dry periods ranged from 0.003 mgL⁻¹ to 4.560 mgL⁻¹, with the lowest 5-year average value being 0.292 mgL⁻¹. The 5-year average contents in flat and rich periods were 0.437 mgL⁻¹ and 0.376 mgL⁻¹, respectively, while their maximum and minimum values were approximately 6.0 mgL⁻¹ and 0.01 mgL⁻¹, respectively. The highest concentration came from Namco every year from 2016 to 2020, exceeding the fluoride limit of 1 mgL⁻¹ in the "Standards for drinking water quality" (GB5749, 2006) and the fluoride limit of 1.5 mgL⁻¹ in the "Standards for surface water quality" (GB3838, 2002) of China.

Table 2 Overall statistics of fluoride concentration in surface water of the TP from 2016 to 2020.

Year	Average (mgL ⁻¹)	Max (mg·L ⁻¹)	Min (mgL ⁻¹)	Standard deviation	Median (mgL ⁻¹)	Sample sizes (N)
2016	0.408	4.730	0.010	0.663	0.238	623
2017	0.359	4.830	0.003	0.653	0.236	814
2018	0.368	6.080	0.003	0.738	0.231	544
2019	0.333	6.240	0.006	0.777	0.245	446
2020	0.278	4.091	0.006	0.597	0.179	270

Table 3 Fluoride concentration in dry, flat and rich periods on the TP.

Parameters	5-year average (mgL ⁻¹)	Max (mgL ⁻¹)	Min (mgL ⁻¹)	Median (mgL ⁻¹)	Standard deviation	Sample sizes (N)
Dry period	0.381	4.560	0.003	0.227	0.612	1079
Flat Period	0.366	6.240	0.009	0.227	0.621	777
Rich period	0.395	6.080	0.013	0.226	0.728	841

3.1.1. Spatial differentiation of surface water fluoride in the Tibetan Plateau

Our results showed that the TP surface water quality displayed spatial variation among the 10 water basins. Sampling sites were set according to the population and water basins. Therefore, the number of sampling sites were unevenly distributed among water basins. For example, 32% of the sampling sites were in the Brahmaputra Basin, compared with barely 3% in the Inner Basin (Fig. 2).

To analyse the characteristics of surface water fluoride in the TP, we divided the water basins into three categories according to the location of the sampling sites and the distance between sampling sites, the main river stream and the population areas: (1) Uniform type, including Brahmaputra, Ganges, Indus, Salween, Yangtze and Yellow River Basins. The sampling sites covered the main stream and densely populated areas and represented the whole water basin well. (2) Scatter type, containing the Hexi, Mekong, and Qaidam Basins. The sampling sites in this type were few and scattered and did not fully cover the densely populated areas. (3) Inner type, a separate classification of the Inner Basin according to its inner lake density, river scarcity, and underpopulation.

The mean concentrations of the water basins were in the following order: Inner > 1 mg L⁻¹ > Qaidam > Mekong > Salween > Yellow River > Indus > Yangtze > Brahmaputra > Hexi > Ganges.

As shown in Fig. 3, the surface water fluoride in the Uniform-type region was lower than 0.50 mg L^{-1} . However, various spatial distributions were shown among water basins. The fluoride concentration in the Salween Basin remained evenly distributed at approximately 0.30 mg L^{-1} , while that in the Brahmaputra Basin was unevenly distributed, with concentrations under 0.25 mg L^{-1} upstream and downstream and relatively higher concentrations in the central region (approximately 0.4 mg L^{-1}). The southwestern region of the TP, where the Indus and Ganges Basins are located, mainly had low values ($< 0.25 \text{ mg L}^{-1}$). The values of two important water basins in China, the Yellow River and Yangtze River, were also under the fluoride limit of the SDWQ.

In the Scatter-type regions, sampling sites were concentrated in the middle and lower reaches of the Mekong Basin in our study area, which had concentrations ranging from 0.25 mg L^{-1} to 0.5 mg L^{-1} . The smallest basin in this study was Hexi. Although there was only one sampling site there, it maintained quite a low value ($< 0.25 \text{ mg L}^{-1}$). The landscape of the Qaidam Basin is an arid desert, and the waters there are mainly inner lakes and their inflows. According to our research, the fluoride concentration in the south-central Qaidam Basin ranged from 0.25 mg L^{-1} to 1.00 mg L^{-1} .

Extremely high values appeared in the Inner-type region, where surface water was sampled at two typical inner lakes (Namco and Siling Co). Fig. 3 shows the water fluoride concentration in the Namco. Consistent with a study by Zhang et al. (Zhang et al., 2008), the concentration of the major ions in the Namco's water was higher than that in the stream water.

The fluoride concentration in lakes was higher than that in rivers in the TP in this study, with average values of 1.36 mg L^{-1} and 0.29 mg L^{-1} , respectively. Five typical lakes (Yamzhog Yumco, Longyangxia Reservoir, Bangong Co, Namco and Siling Co) in this study were taken into consideration to explore large differences between lake and river concentrations. We analysed rivers, lakes and lake-inflows in the same water basin according to their flow direction and confluence area. Fig. 4 clearly shows that fluoride concentrations in lakes were higher than rivers and lake-inflows in the same water basin. The fluoride concentrations in the Yamzhog Yumco and Longyangxia Reservoirs, with average values of 0.64 mg L^{-1} and 0.35 mg L^{-1} , respectively, were 2-3 times higher than those in their inflows. Meanwhile, the average values of rivers in the Brahmaputra, Yellow River and Indus Basins remained at approximately 0.2 mg L^{-1} . The mean (4.11 mg L^{-1}) and median (4.28 mg L^{-1}) fluoride concentrations in the Namco were considerably high. Compared to rivers, the other typical lake (Siling Co) in the Inner Basin also had a considerably high average concentration (0.61 mg L^{-1}).

Studies related to fluoride in surface water in the TP published from 2010–2021 were collected, including fluoride data in a total of 18 lakes and 18 rivers (Table 4). It clearly shown that fluoride concentration in lakes were exceedingly higher than it in rivers. In addition, a comparison between the three inner lakes (Yamzhog Yumco, Namco, and Qinhai Lake) and their inflows showed that fluoride concentrations were concentrated after water flowed into the lake (Fig. 5), which was consistent with our study.

There may be several influencing factors according to the literature. Evaporation plays a certain role in the increase in ions in lake water (Wang et al., 2020). The lakes in the TP are mainly inland; thus, fluoride is concentrated in the lakes as water evaporates. It has also been reported that the water ion composition of the Nam Co is dominated by evaporation and crystallization (Ma et al., 2016). The geological conditions of confluence and rock weathering affect river water ion concentrations (Yu et al., 2021). Additionally, weathering is a main factor causing the increase in all ions in the lake water and most ions in the river water (Wu et al., 2016). According to the existing research on water in the TP, the chemical composition changed after the river flowed into the lake, and the main positive ions changed from $(\text{Ca}^+ + \text{Mg}^+)$ to $(\text{Na}^+ + \text{Mg}^+)$ (Wang et al., 2010). Water F^- was positively correlated with Na^+ and presented a significantly negative relationship with Ca^{2+} (Liu et al., 2021). A series of complex chemical processes occurred in the lake water, accumulating fluoride to some extent.

Table 4 Fluoride concentration in lakes and rivers in the TP (mg L^{-1})

Lake			River		
Pengco	5.53	Yan et al., 2018	Yairuzangbo	0.42	An et al., 2017
Bangeco	0.47	Yan et al., 2018	Yajian river	0.382	Zhe et al., 2016
Yagenco	0.66	Yan et al., 2018	Puzong river	0.154	Qu et al., 2017
Siling Co	0.50	Yan et al., 2018	Xiangda river	0.197	Qu et al., 2017
Xueyuanco	5.45	Yan et al., 2018	Gamalin river	0.214	Qu et al., 2017
Dawaco	1.43	Yan et al., 2018	Kaluxiong river	0.2	Qu et al., 2017
Dajiaco	24.35	Yan et al., 2018	Kadongjia river	0.162	Qu et al., 2017
Qiduoco	0.21	Yan et al., 2018	Quqing river	0.184	Qu et al., 2017
Angren lake	16.36	Yan et al., 2018	Inflow of Namco	0.38	Wang et al., 2010
Langco	0.74	Yan et al., 2018	Buha river	0.2	Jin et al., 2010
Gahai	1.15	Yan et al., 2018	Yairuzangbo	0.16	Liu et al., 2018
Yamzhog yumco	0.69	Zhang et al., 2012	Maqu	0.23	Li et al., 2020
Pumo yumco	0.83	Zhang et al., 2012	Chumaer river	0.5	Jiang et al., 2015
Chenco	0.81	Zhang et al., 2012	Tuotuo river	0.35	Jiang et al., 2015
Kongmuco	0.14	Zhang et al., 2012	Dang river	0.21	Jiang et al., 2015
Bajiuco	1.12	Zhang et al., 2012	Zhimenda	0.17	Jiang et al., 2015
Yamzhog yumco	0.82	Qu et al., 2017	Shaliu river	0.31	Ji et al., 2021
Pumo yumco	0.83	Qu et al., 2017	Palongzangbo	0.18	Zhang et al., 2020
Chenco	0.97	Qu et al., 2017			
Kongmuco	0.20	Qu et al., 2017			
Bajiuco	1.08	Qu et al., 2017			
Mapang yumco	1.17	Wang et al., 2010			
Laangco	2.98	Wang et al., 2010			
Namco	5.79	Wang et al., 2010			
Qinhai Lake	1.00	Tian et al., 2019			
Qinhai Lake	7.60	Zhang et al., 2010			
Yamzhog yumco	0.66	Tian et al., 2019			
Namco	4.02	Tian et al., 2019			

3.1.2. Temporal differentiation of surface water fluoride in the Tibetan Plateau

Regarding the timeline changes in fluoride concentration, our analysis showed that the fluoride concentration in the three different periods (dry period, flat period, and rich period) remained relatively stable, changing little in general. However, there were still some variabilities. The fluoride concentration in the whole Ganges Basin showed a higher value (0.25 mg L^{-1} – 0.50 mg L^{-1}) in the flat period of 2018 than in other periods during 2016–2020. In areas with a high population density, such as the central Brahmaputra Basin, the northeastern Yellow River Basin, and the middle Mekong Basin, the fluoride concentration in the three periods of 2020 presented a lower value than that in the same periods during 2016–2019. This may have been due to decreases in anthropogenic activities in 2020 due to COVID-19, illustrating that anthropogenic activities may affect surface water fluoride.

In addition, there was a downwards tendency in fluoride concentration each year. For instance, Fig. 6 shows that fluoride concentrations in the Yellow River Basin during all three water periods had an obvious declining trend. The lake fluoride value showed the same decrease, which may be related to the increase of lake water storage caused by climate change (Zhu et al., 2020; Yan et al., 2018). Researchers have also revealed that major ions decreased in response to regional climatic change in Tibetan lakes (Qiao et al., 2019).

3.2. Effects of anthropogenic factors and natural characteristics on surface water fluoride

To identify the influence of anthropogenic, climate condition, and topographical factors on surface water fluoride, Pearson's rank correlation analysis was conducted for surface water fluoride content in 8 different basins (Brahmaputra, Ganges, Indus, Mekong, Qaidam, Salween, Yangtze, and Yellow River) and 5 key factors (night-light intensity, air temperature, elevation, precipitation, and slope), while the Hexi and Inner Basins were eliminated due to few sampling sites (Table 6).

The night light index, which is used to measure the intensity of anthropogenic activities, has been widely used in the field of environmental sciences (Zheng et al., 2022). Therefore, the night light index was used to represent the influence of anthropogenic activities in our study. The contrast between bright and dark areas in night-light images makes it a powerful tool to study intensive anthropogenic activities and their effects (Stathakis et al., 2018). Night light intensity showed a positive relationship with fluoride concentration in high population density areas (Brahmaputra, Mekong, Salween, and Yellow River Basins). In particular, the correlations in the Brahmaputra and Salween Basins were 0.477 and 0.972, respectively ($P < 0.05$). The results suggest that anthropogenic activities may increase the water fluoride concentration in high population density areas on the TP.

Concerning regional climate, surface water fluoride concentration had a weakly negative relationship with precipitation and an insignificant positive relationship with elevation, while air temperature was

negatively related to surface water fluoride ($r = -0.296$, $P < 0.05$). Precipitation was negatively related to fluoride in nearly all the water basins. During precipitation, water inflows via surface and subsurface processes from soil and thus may significantly modulate water quality and ion concentration (Wu et al., 2019). Therefore, precipitation intensity and frequency directly affect water quality. Air temperature was positively correlated with fluoride in the northeastern area but negatively related in the remaining areas. Water temperature changes with air temperature changes. Generally, air temperature can affect the density, surface tension, viscosity and morphology of water bodies and change the distribution of the water temperature layer, the rate of chemical reaction and biodegradation in water bodies, which fundamentally controls the physical and chemical properties and biological characteristics of the water bodies (Giri et al., 2021).

Among numerous topographical factors, surface elevation and slope were the most essential and were recognized as the key factors (Xu et al., 2018). As for the relationship between elevation and fluoride, the southeastern TP, including the Mekong ($r = 0.646$), Salween ($r = 0.301$), and Yangtze ($r = 0.955$, $P < 0.05$) Basins, presented a significantly positive relationship. These three basins are close to the first and second steps of China's terrain, with rapid terrain declines and efficient water confluence resulting in a diluted fluoride concentration. However, the northeastern TP (Yellow River and Qaidam Basins) revealed a negative but unobvious correlation. The slope showed negative but insignificant correlations with water basins.

Table 5 Pearson's rank correlation coefficients of anthropogenic and natural drivers to the fluoride at nine major river basins in TP

Correlation	Night light intensity	Air temperature	Precipitation	Elevation	Slope
All basins	0.043	-.296*	-0.158	0.172	0.003
Brahmaputra	0.477*	-0.323	-0.241	-0.178	0.175
Ganges	-0.716	-0.116	-0.214	0.077	-0.479
Indus	-0.452	-0.241	0.169	-0.132	-0.341
Mekong	0.386	-0.118	-0.216	0.646	-0.226
Qaidam	-0.124	0.769	-0.729	-0.791	-0.337
Salween	0.972*	-0.557	-0.673	0.301	0.278
Yangtze	-0.103	-0.571	-0.443	0.955*	-0.826
Yellow River	0.255	0.225	-0.540*	-0.312	0.225
*P < 0.05					

3.3. Health risk of fluoride in surface water in the Tibetan Plateau

3.3.1. Health risk assessment

The health risk attributable to fluoride varied by absorption approach, age and water period (Table 6). The HR value via the ingestion absorption pathway ranged from 0.07 to 0.37, while the health risk via the dermal absorption pathway was low ($0.50 \times 10^{-4} < HR < 1.39 \times 10^{-4}$). The highest water health risk was associated with the dry periods, followed by the rich periods and the flat periods. With little variation among water periods, the dry period lasts the longest in a year and pose the highest health risks. From an age group perspective, infants and adults suffered more health risks, while the HR value for teenagers was significantly lower than that for other age groups. Overall, the average health risk was quite low ($HR < 1$) and had a small impact on health.

Table 6 HR values for the five age groups.

		Rich period	Flat period	Dry period	Average
Ingesting Health Risk	Infant (0-3)	0.12	0.09	0.16	0.37
	Young Children (4-6)	0.09	0.07	0.13	0.29
	Children (7-12)	0.08	0.06	0.12	0.26
	Teenager (13-18)	0.07	0.05	0.10	0.22
	Adults (>18)	0.11	0.08	0.16	0.36
Dermal Health Risk ($\times 10^{-4}$)	Infant (0-3)	0.54	0.50	0.52	0.51
	Young Children (4-6)	0.80	0.74	0.77	0.76
	Children (7-12)	0.63	0.58	0.60	0.60
	Teenager (13-18)	1.39	1.29	1.34	1.33
	Adults (>18)	1.13	1.05	1.09	1.08

Figure 8 presents the fluoride health risk distribution of TP water basins by age group. The lowest health risk was associated with nearly all age groups in the Hexi Basin, where the HR value ranged from 0.11 to 0.18. The health risk in the Inner Basin remained the highest for all age groups, especially for infants and adults ($HR > 3$).

3.3.2. Sensitivity analyses

Uncertainties in the distribution of surface water fluoride concentration, concentration–response functions and valuation methods affected the health risk estimates. Monte Carlo simulations were adopted to estimate 95% uncertainty intervals from 5000 draws of parameters and concentrations

throughout the health risk assessment (Yin et al., 2021). The Crystal Ball software was used for simulation and sensitivity analysis to determine the variables contributing to the health risk assessment.

The correlation coefficients of fluoride concentration and concentration–response function parameters are shown in Fig. 9. The drink rate (IR) and concentration (C) contributed the most (over 90%) to both ingestion and dermal absorption, while the exposure frequency had little influence in all age groups. The correlation coefficients of body weight (BW) were similar for the two pathways in the same age groups, with values of approximately 3.75% for infants, 3% for young children, 7% for children, 4% for teenagers and 5% for adults.

3.3.3. Potential affected population

More than 70% of the population in the TP inhabits uniform type areas. Approximately 20% of the population in the TP lives in the scatter type areas, while barely 200 thousand residents are spread throughout the inner type areas (Fig. 10). To calculate how many people are exposed within the sampling range, we added population data from all the towns within 5 km of a sampling site. Approximately 300 thousand residents live within 5 km of a sampling site in the scatter type areas, and approximately 50 thousand residents live within 5 km of a sampling lake in the inner type areas.

For the uniform type areas, the sampling sites covered the main stream and densely populated areas, which can well represent the fluoride of the whole basin. The population in both the uniform type areas and the scatter type areas had a low health risk, which means that more than 75% of the population on the TP was safe in terms of surface water fluoride. However, residents living near the Namco and Seling Co were more likely to suffer diseases related to fluoride. As analysed above, the fluoride concentration in the lakes was generally high ($>1 \text{ mg L}^{-1}$) in the TP, and the inner lake was the main water body in the inner type areas. It is obvious that residents in the inner type areas suffered a high health risk and had a strong possibility of contracting diseases. With barely 200 thousand permanent residents, the Inner Basin is one of the least densely populated regions in the TP. Furthermore, residents living near lakes in other regions of the TP also suffered a relatively high health risk in this study. This should be taken seriously, and the government needs to adopt safety measures for all inner lakes in the TP.

As analysed above, the fluoride concentration and health risk of rivers remained at a low level. The confluence area of the river increases as the river flows, the proportion of new water in the total water becomes increasingly higher, and the fluoride from the source water is diluted. Therefore, the fluorosis in downstream areas had little relation to the water resources in the TP. According to the relevant literature, India, China and other downstream areas have shown varying degrees of fluorosis. Whether the existing low fluorine content in the source water will play a role in the fluorosis caused by other factors downstream needs to be further studied.

4. Conclusion

The fluoride concentration in surface water in the TP ranged from 0.005 mg L⁻¹ to 6.240 mg L⁻¹. The spatial distribution was in the following order: Inner > 1 mg L⁻¹ > Qaidam > Mekong > Salween > Yellow River > Indus > Yangtze > Brahmaputra > Hexi > Ganges; and lakes > rivers. No appreciable change in fluoride concentrations among dry, flat, and rich periods was observed; however, a tendency for decreasing fluoride levels with increasing years in the surface water in the TP was obviously present.

In general, the fluoride concentration in the surface water in the TP was positively related to anthropogenic activities and was negatively correlated with regional climate factors, including precipitation and air temperature, which was consistent with our results showing that the fluoride concentration decreased by year. The topography showed an uncertain relationship. Consequently, the distribution of the fluoride concentration in the surface water in TP is compounded by antagonistic and synergistic effects of various factors, but the specific mechanism of this compound influence needs to be further studied.

The health risk by ingestion was higher than that by dermal absorption, with values of 0.07–0.37 and 0.50×10^{-4} <HR < 1.39×10^{-4} , respectively. The drink rate and concentration contributed more than 90% to the sensitivity of the health risk for both ingestion and dermal absorption. Unacceptable surface water health risks barely occurred in the Inner Basin and regions near the lake, and more than 75% of the population in the TP was safe in terms of surface water fluoride. Although surface water is not the main cause of fluorosis, it should be taken seriously. Fluoride accumulates in humans, and an increase in surface water fluoride intake can aggravate serious fluorosis in the TP, which has not been addressed in previous studies.

Nevertheless, our study has some limitations, and further research is needed. First, although the water sampling data in our study cover the main streams and typical lakes of the TP, due to the large number of tributaries, it is not yet possible to represent the water quality of the region with a high accuracy. In addition, there are many other sources of human fluoride intake in addition to surface water, such as groundwater and meltwater, which may result in an underestimation of the risk posed by total water fluoride to human health. Therefore, it should be noted that the present study may have underestimated the risk posed by water fluoride to human health in the plateau area.

Declarations

Acknowledgements

This work was supported by the Second Tibetan Plateau Scientific Expedition and Research Program (No. 2019QZKK0607) and National Science Foundation of China (No. 420774280).

Competing Interests

The authors have no relevant financial or non-financial interests to disclose.

Authorship contribution statement

All authors contributed to the study conception and design. **Yi Yang**: Methodology, Visualization, Writing - original draft; **Ru Zhang**: Data analysis; **Fengying Zhang**: Data curation, Writing – review & editing; **Yonghua Li**: Conceptualization, Supervision, Funding acquisition. All authors read and approved the final manuscript.

Data Availability

The datasets generated during and/or analysed during the current study are not publicly available due to no datasets were generated or analysed during the current study, all data sources shown in supplementary material.

References

1. Ahada, C.P.S., Suthar, S., 2019. Assessment of human health risk associated with high groundwater fluoride intake in southern districts of Punjab, India. *Expo. Health* 11, 267–275. <https://doi.org/10.1007/s12403-017-0268-4>.
2. An, L., Yao, X., Yang, D., Sun, M., Qi, M., Gong, P., Li, X., Gao, Y., 2017. Major ions and their controlling factors of surface water in the northern slopere region in the middle Himalayas: a case study of Yairuzangbo Basin. *Acta Sci. Circumst.* 37, 2524–2530. <https://doi.org/10.13671/j.hjkxxb.2017.0047> (in Chinese).
3. Dong, L., Tang, S., Cosh, M.H., Zhao, P., Lu, P., Zhou, K., Han, S., Min, M., Xu, N., Chen, L., Wang, F., 2020. Studying soil moisture and temperature on the Tibetan Plateau: initial results of an integrated, multiscale observatory. *IEEE Geosci. Remote Sens. Mag.* 8, 18–36. <https://doi.org/10.1109/MGRS.2019.2924678>.
4. Duan, Q., Duan, A., 2020. The energy and water cycles under climate change. *Natl. Sci. Rev.* 7, 553–557. <https://doi.org/10.1093/nsr/nwaa003>.
5. Duan, X., 2012. Highlights of the Chinese Exposure Factors Handbook (Adults). China Environmental Science Press, Beijing.
6. Duan, X., 2012. Highlights of the Chinese Exposure Factors Handbook (Children). China Environmental Science Press, Beijing.
7. GB 19965, 2005. Fluoride content of brick tea. National standards of the People's Republic of China.
8. GB 3838, 2002. Standards for surface water quality. National standards of the People's Republic of China.
9. GB 5749, 2006. Standards for drinking water quality. National standards of the People's Republic of China.
10. Giri, S., 2021. Water quality prospective in Twenty First Century: Status of water quality in major river basins, contemporary strategies and impediments: a review. *Environ. Pollut.* 271, 116332. <https://doi.org/10.1016/j.envpol.2020.116332>.

11. Hettithanthri, O., Sandanayake, S., Magana-Arachchi, D., Wanigatunge, R., Rajapaksha, A.U., Zeng, X., Shi, Q., Guo, H., Vithanage, M., 2021. Risk factors for endemic chronic kidney disease of unknown etiology in Sri Lanka: Retrospect of water security in the dry zone. *Sci. Total Environ.* 795, 148839. <https://doi.org/10.1016/j.scitotenv.2021.148839>.
12. Ji, Y., Cao, S., Cao, G., Li, H., 2020. Hydrochemical characteristics of river water and groundwater in Shaliu river basin of Qinghai Lake in summer. *J. Qinghai Norm. Univ.* 37, 63–75 (in Chinese).
13. Jiang, L., Yao, Z., Liu, Z., Wang, R., Wu, S., 2015. Hydrochemistry and its controlling factors of rivers in the source region of the Yangtze River on the Tibetan Plateau. *J. Geochem. Explor.* 155, 76–83. <https://doi.org/10.1016/j.gexplo.2015.04.009>.
14. Jin, Z., You, C.-F., Wang, Y., Shi, Y., 2010. Hydrological and solute budgets of Lake Qinghai, the largest lake on the Tibetan Plateau. *Quat. Int., Climate Evolution and Environmental Response on the Tibetan Plateau* 218, 151–156. <https://doi.org/10.1016/j.quaint.2009.11.024>.
15. Li, Y., Bi, Y., Mi, W., Xie, S., Ji, L., 2021. Land-use change caused by anthropogenic activities increase fluoride and arsenic pollution in groundwater and human health risk. *J. Hazard. Mater.* 406, 124337. <https://doi.org/10.1016/j.jhazmat.2020.124337>.
16. Li, ZongJie, Li, ZongXing, Song, L., Gui, J., Xue, J., Zhang, B., Gao, W., 2020. Precipitation chemistry in the Source Region of the Yangtze River. *Atmospheric Res.* 245, 105073. <https://doi.org/10.1016/j.atmosres.2020.105073>.
17. Liu, J., Peng, Y., Li, C., Gao, Z., Chen, S., 2021. A characterization of groundwater fluoride, influencing factors and risk to human health in the southwest plain of Shandong Province, North China. *Ecotoxicol. Environ. Saf.* 207, 111512. <https://doi.org/10.1016/j.ecoenv.2020.111512>.
18. Liu, J., Zhao, Y., Huang, X., Guo, H., 2018. Spatiotemporal variations of hydrochemistry and its controlling factors in the Yarlung Tsangpo River. *China Environ. Sci.* 2018, 4289–4297. <https://doi.org/10.19674/j.cnki.issn1000-6923.2018.0479>.
19. Liu, S., Yao, Y., Kuang, X., Zheng, C., 2021. A preliminary investigation on the climate-discharge relationship in the upper region of the Yarlung Zangbo River basin. *J. Hydrol.* 603, 127066. <https://doi.org/10.1016/j.jhydrol.2021.127066>.
20. Liu, Y., Yang, Y., Wei, Y., Liu, X., Li, B., Chu, Y., Huang, W., Wang, L., Lou, Q., Guo, N., Wu, L., Wang, J., Zhang, M., Yin, F., Fan, C., Su, M., Zhang, Z., Zhang, X., Gao, Y., Sun, D., 2020. Sklotho is associated with the severity of brick tea-type skeletal fluorosis in China. *Sci. Total Environ.* 744, 140749. <https://doi.org/10.1016/j.scitotenv.2020.140749>.
21. Lou, Q., Guo, N., Huang, W., Wu, L., Su, M., Liu, Y., Liu, X., Li, B., Yang, Y., Gao, Y., 2021. Association between bone morphogenetic protein 2 gene polymorphisms and skeletal fluorosis of the brick-tea type fluorosis in Tibetans and Kazakhs, China. *Int. J. Environ. Health Res.* 0, 1–11. <https://doi.org/10.1080/09603123.2021.1892037>.
22. Lu, P., Han, J., Li, Z., Xu, R., Li, R., Hao, T., Qiao, G., 2020. Lake outburst accelerated permafrost degradation on Qinghai-Tibet Plateau. *Remote Sens. Environ.* 249, 112011. <https://doi.org/10.1016/j.rse.2020.112011>.

23. Ma, F., Chen, Jiaqi, Chen, Jiansheng, Wang, T., Han, L., Zhang, X., Yan, J., 2021. Evolution of the hydro-ecological environment and its natural and anthropogenic causes during 1985–2019 in the Nenjiang River basin. *Sci. Total Environ.* 799, 149256. <https://doi.org/10.1016/j.scitotenv.2021.149256>.
24. Ma, N., Szilagyi, J., Niu, G.Y., Zhang, Y., Zhang, T., Wang, B., Wu, Y., 2016. Evaporation variability of Nam Co Lake in the Tibetan Plateau and its role in recent rapid lake expansion. *J. Hydrol.* 537, 27–35. <https://doi.org/10.1016/j.jhydrol.2016.03.030>.
25. Meng, X., Yao, Y., Ma, Y., Zhong, N., Alphonse, S., Pei, J., 2021. Effect of fluoride in drinking water on the level of 5-methylcytosine in human and rat blood. *Environ. Toxicol. Pharmacol.* 81, 103511. <https://doi.org/10.1016/j.etap.2020.103511>.
26. Narsimha, A., Rajitha, S., 2018. Spatial distribution and seasonal variation in fluoride enrichment in groundwater and its associated human health risk assessment in Telangana State, South India. *Hum. Ecol. Risk Assess. Int. J.* 24, 2119–2132. <https://doi.org/10.1080/10807039.2018.1438176>.
27. Nury, A.H., Sharma, A., Marshall, L., Cordery, I., 2021. Modelling climate change impacts on the Brahmaputra streamflow resulting from changes in snowpack attributes. *J. Hydrol.* 603, 126998. <https://doi.org/10.1016/j.jhydrol.2021.126998>.
28. Pi, X., Feng, L., Li, W., Zhao, D., Kuang, X., Li, J., 2020. Water clarity changes in 64 large alpine lakes on the Tibetan Plateau and the potential responses to lake expansion. *ISPRS J. Photogramm. Remote Sens.* 170, 192–204. <https://doi.org/10.1016/j.isprsjprs.2020.10.014>.
29. Qiao, B., Nie, B., Liang, C., Xiang, L., Zhu, L., 2021. Spatial Difference of Terrestrial Water Storage Change and Lake Water Storage Change in the Inner Tibetan Plateau. *Remote Sens.* 13, 1984. <https://doi.org/10.3390/rs13101984>.
30. Qu, B., Zhang, Y., Kang, S., Sillanpää, M., 2017. Water chemistry of the southern Tibetan Plateau: an assessment of the Yarlung Tsangpo river basin. *Environ. Earth Sci.* 76, 1–12. <https://doi.org/10.1007/s12665-017-6393-3>.
31. Ran, F., Nie, X., Li, Zhongwu, Xiao, L., Sun, Y., Wang, S., Liao, W., Tong, D., Li, Zeting, Peng, Y., 2021. Chronological records of sediment organic carbon at an entrance of Dongting Lake: Response to historical meteorological events. *Sci. Total Environ.* 794, 148801. <https://doi.org/10.1016/j.scitotenv.2021.148801>.
32. Stathakis, D., Baltas, P., 2018. Seasonal population estimates based on night-time lights. *Comput. Environ. Urban Syst.* 68, 133–141. <https://doi.org/10.1016/j.compenvurbsys.2017.12.001>.
33. Tian, Y., Yu, C., Zha, X., Gao, X., Dai, E., 2019. Hydrochemical characteristics and controlling factors of natural water in the border areas of the Qinghai-Tibet Plateau. *J. Geogr. Sci.* 29, 1876–1894. <https://doi.org/10.1007/s11442-019-1994-y>.
34. USEPA, 1989. EPA/540/1-89/002. Risk assessment guidance for superfund volume 1—Human health evaluation manual (Part A). Washington DC.
35. USEPA, 2008. EPA/600/R-06/096F. Child-Specific Exposure Factors Handbook. Washington DC.

36. Wang, B., Ma, Y., Su, Z., Wang, Y., Ma, W., 2020. Quantifying the evaporation amounts of 75 high-elevation large dimictic lakes on the Tibetan Plateau. *Sci. Adv.* 6, eaay8558.
<https://doi.org/10.1126/sciadv.aay8558>.
37. Wang, J., Zhao, S., Yang, L., Gong, H., Li, H., Nima, C., 2020. Assessing the Health Loss from Kashin-Beck Disease and Its Relationship with Environmental Selenium in Qamdo District of Tibet, China. *Int. J. Environ. Res. Public Health* 18, E11. <https://doi.org/10.3390/ijerph18010011>.
38. Wang, J., Zhu, L., Wang, Y., Ju, J., Xie, M., Daut, G., 2010. Comparisons between the chemical compositions of lake water, inflowing river water, and lake sediment in Nam Co, central Tibetan Plateau, China and their controlling mechanisms. *J. Gt. Lakes Res.* 36, 587–595.
<https://doi.org/10.1016/j.jglr.2010.06.013>.
39. Wang, W., Zheng, W., Zhang, P., Li, Q., Kirby, E., Yuan, D., Zheng, D., Liu, C., Wang, Z., Zhang, H., Pang, J., 2017. Expansion of the Tibetan Plateau during the Neogene. *Nat. Commun.* 8, 15887.
<https://doi.org/10.1038/ncomms15887>.
40. Wang, Y., Wang, L., Li, X., Zhou, J., Hu, Z., 2020. An integration of gauge, satellite, and reanalysis precipitation datasets for the largest river basin of the Tibetan Plateau. *Earth Syst. Sci. Data* 12, 1789–1803. <https://doi.org/10.5194/essd-12-1789-2020>.
41. Wu, S., Yin, Y., Zheng, D., Yang, Q., 2007. Climatic trends over the Tibetan Plateau during 1971–2000. *J. Geogr. Sci.* 17, 141–151. <https://doi.org/10.1007/s11442-007-0141-7>.
42. Wu, W., 2016. Hydrochemistry of inland rivers in the north Tibetan Plateau: Constraints and weathering rate estimation. *Sci. Total Environ.* 541, 468–482.
<https://doi.org/10.1016/j.scitotenv.2015.09.056>.
43. Wu, Y., Guo, L., Zheng, H., Zhang, B., Li, M., 2019. Hydroclimate assessment of gridded precipitation products for the Tibetan Plateau. *Sci. Total Environ.* 660, 1555–1564.
<https://doi.org/10.1016/j.scitotenv.2019.01.119>.
44. Xu, F., Zhang, G., Yi, S., Chen, W., 2021. Seasonal trends and cycles of lake-level variations over the Tibetan Plateau using multi-sensor altimetry data. *J. Hydrol.* 127251.
<https://doi.org/10.1016/j.jhydrol.2021.127251>.
45. Xu, Y., Li, Y., Li, H., Wang, L., Liao, X., Wang, J., Kong, C., 2018. Effects of topography and soil properties on soil selenium distribution and bioavailability (phosphate extraction): a case study in Yongjia County, China. *Sci. Total Environ.* 633, 240–248.
<https://doi.org/10.1016/j.scitotenv.2018.03.190>.
46. Yan, L., Sun, M., Yao, X., Gong, N., Li, X., Qi, M., 2018. Lake water in the Tibet Plateau: quality change and current status evaluation. *Acta Sci. Circumst.* 38, 900–910.
<https://doi.org/10.13671/j.hjkxxb.2017.0390>.
47. Yang, K., He, J., 2019. China meteorological forcing dataset (1979-2018). National Tibetan Plateau Data Center. <https://doi.org/10.11888/AtmosphericPhysics.tpe.249369>.
48. Yin, N., Li, Yunpeng, Yang, Y., Fan, C., Li, Yan, Du, X., Sun, G., Cui, Y., 2021. Human health risk assessment in aluminium smelting site: Soil fluoride bioaccessibility and relevant mechanism in

- simulated gastrointestinal tract. *J. Hazard. Mater.* 416, 125899. <https://doi.org/10.1016/j.jhazmat.2021.125899>.
49. Yin, Z., Luo, Q., Wu, Jianfeng, Xu, S., Wu, Jichun, 2021. Identification of the long-term variations of groundwater and their governing factors based on hydrochemical and isotopic data in a river basin. *J. Hydrol.* 592, 125604. <https://doi.org/10.1016/j.jhydrol.2020.125604>.
50. Yu, Z., Wu, G., Li, F., Huang, J., Xiao, X., Liu, K., 2021. Small-catchment perspective on chemical weathering and its controlling factors in the Nam Co basin, central Tibetan Plateau. *J. Hydrol.* 598, 126315. <https://doi.org/10.1016/j.jhydrol.2021.126315>.
51. Li, Y., Wang, F., Feng, J., Lv, J., Liu, Q., Nan, F., Liu, X., Xu, L., Xie, S., 2020. Increased health threats from land use change caused by anthropogenic activity in an endemic fluorosis and arsenicosis area. *Environ. Pollut.* 261, 114130. <https://doi.org/10.1016/j.envpol.2020.114130>.
52. Zhang, G. 2019. Dataset of river basins map over the TP 2016. National Tibetan Plateau Data Center. <https://doi.10.11888/BaseGeography.tpe.249465>.
53. Zhang, G., Yao, T., Chen, W., Zheng, G., Shum, C.K., Yang, K., Piao, S., Sheng, Y., Yi, S., Li, J., O'Reilly, C.M., Qi, S., Shen, S.S.P., Zhang, H., Jia, Y., 2019. Regional differences of lake evolution across China during 1960s–2015 and its natural and anthropogenic causes. *Remote Sens. Environ.* 221, 386–404. <https://doi.org/10.1016/j.rse.2018.11.038>.
54. Zhang, L., Huang, D., Yang, J., Wei, X., Qin, J., Ou, S., Zhang, Z., Zou, Y., 2017. Probabilistic risk assessment of Chinese residents' exposure to fluoride in improved drinking water in endemic fluorosis areas. *Environ. Pollut.* 222, 118–125. <https://doi.org/10.1016/j.envpol.2016.12.074>.
55. Zhang, L., Zhao, L., Zeng, Q., Fu, G., Feng, B., Lin, X., Liu, Z., Wang, Y., Hou, C., 2020. Spatial distribution of fluoride in drinking water and health risk assessment of children in typical fluorosis areas in north China. *Chemosphere* 239, 124811. <https://doi.org/10.1016/j.chemosphere.2019.124811>.
56. Zhang, R., Cheng, L., Zhang, T., Xu, T., Li, M., Yin, W., Jiang, Q., Yang, Y., Hu, T., 2019. Brick tea consumption is a risk factor for dental caries and dental fluorosis among 12-year-old Tibetan children in Ganzi. *Environ. Geochem. Health* 41, 1405–1417. <https://doi.org/10.1007/s10653-018-0216-7>.
57. Zhang, R., Zhu, L., Ma, Q., Chen, H., Liu, C., Zubaida, M., 2021. The consecutive lake group water storage variations and their dynamic response to climate change in the central Tibetan Plateau. *J. Hydrol.* 601, 126615. <https://doi.org/10.1016/j.jhydrol.2021.126615>.
58. Zhang, X., Sun, R., Zhu, L., 2012. Lake water in the Yamzhog Yumco basin in south Tibetan region: quality and evaluation. *J. Glaciol Geocryol.* 34, 950–958 (in Chinese).
59. Zheng, Y., He, Y., Zhou, Q., Wang, H., 2022. Quantitative evaluation of urban expansion using NPP-VIIRS nighttime light and Landsat spectral data. *Sustain. Cities Soc.* 76, 103338. <https://doi.org/10.1016/j.scs.2021.103338>.

Figures

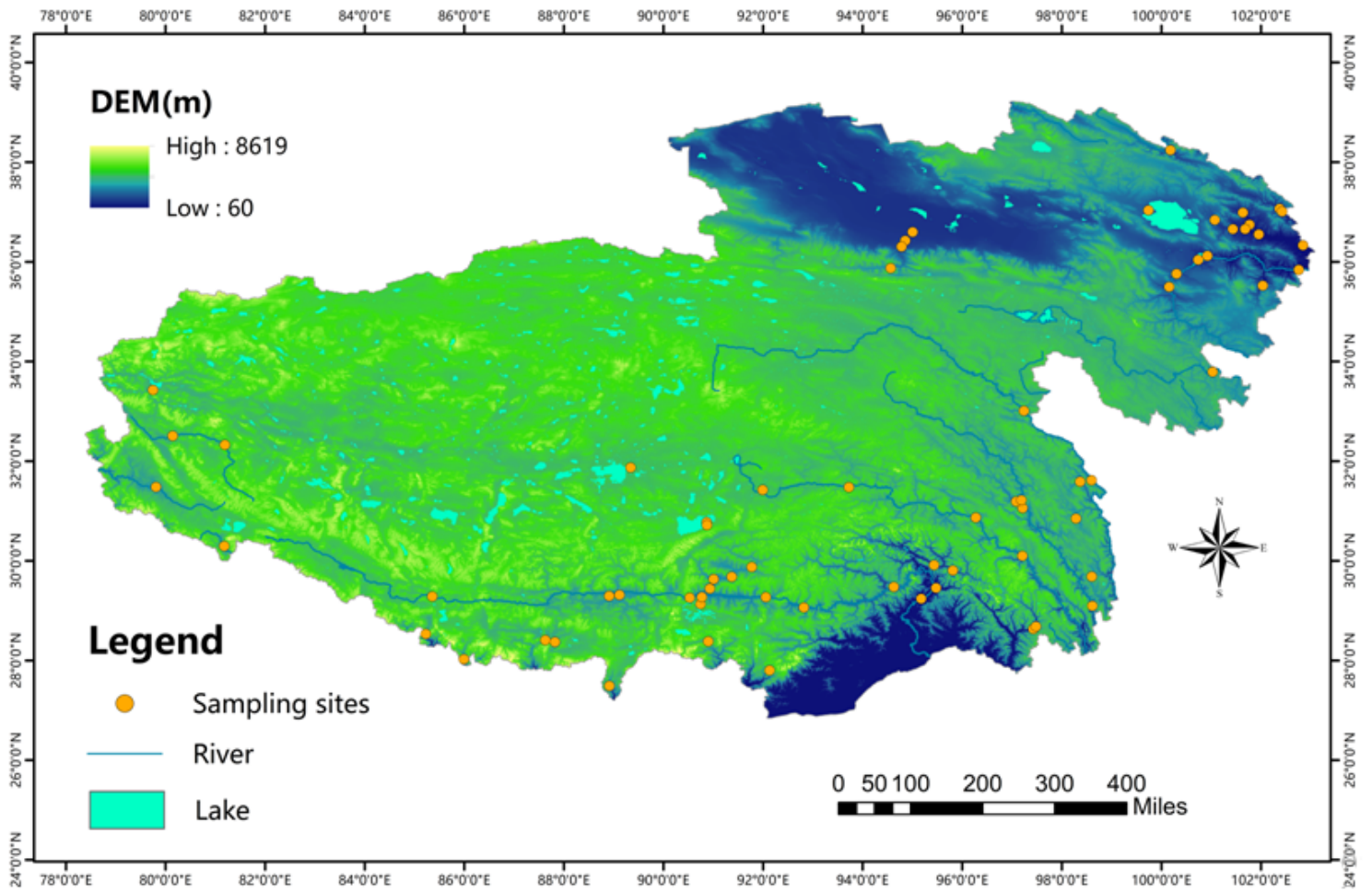


Figure 1

Spatial distribution of national monitoring stations in the TP surface waters.

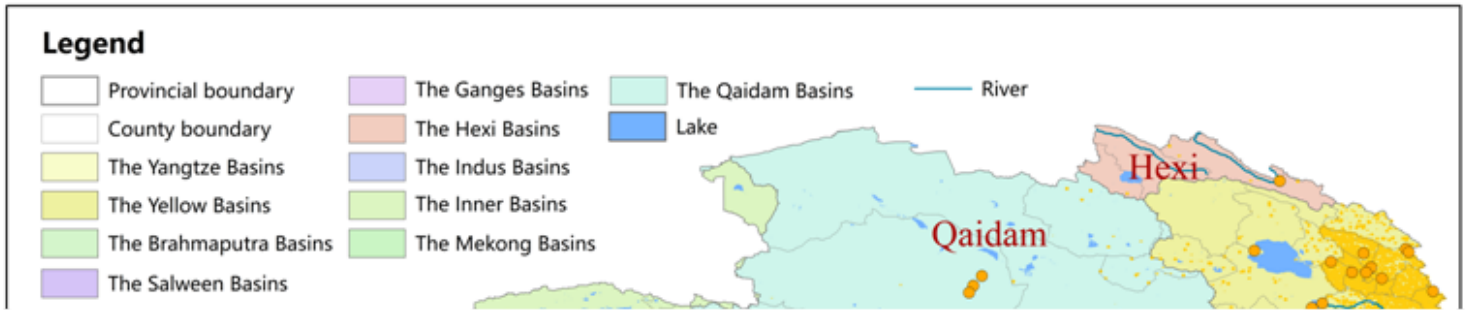


Figure 2

Water basins and population density.

Figure 3

Spatial patterns of annual average and 5-year average water fluoride in the TP during 2016–2020.

Figure 4

Sampling distribution and boxplot of fluoride in different water basins among rivers, lakes and inflows.

Figure 5

Fluoride concentration in lakes and their inflows from existing research.

Figure 6

Variability in water fluoride in dry, flat, and rich periods during 2016–2020.

Figure 7

Distribution of the night light index, air temperature, precipitation, and slope, and spatial interpolation of fluoride concentration.

Figure 8

Health risk by age in different basins.

Figure 9

Sensitivity analysis of age groups for health risk assessment of surface water ingestion and dermal contact.

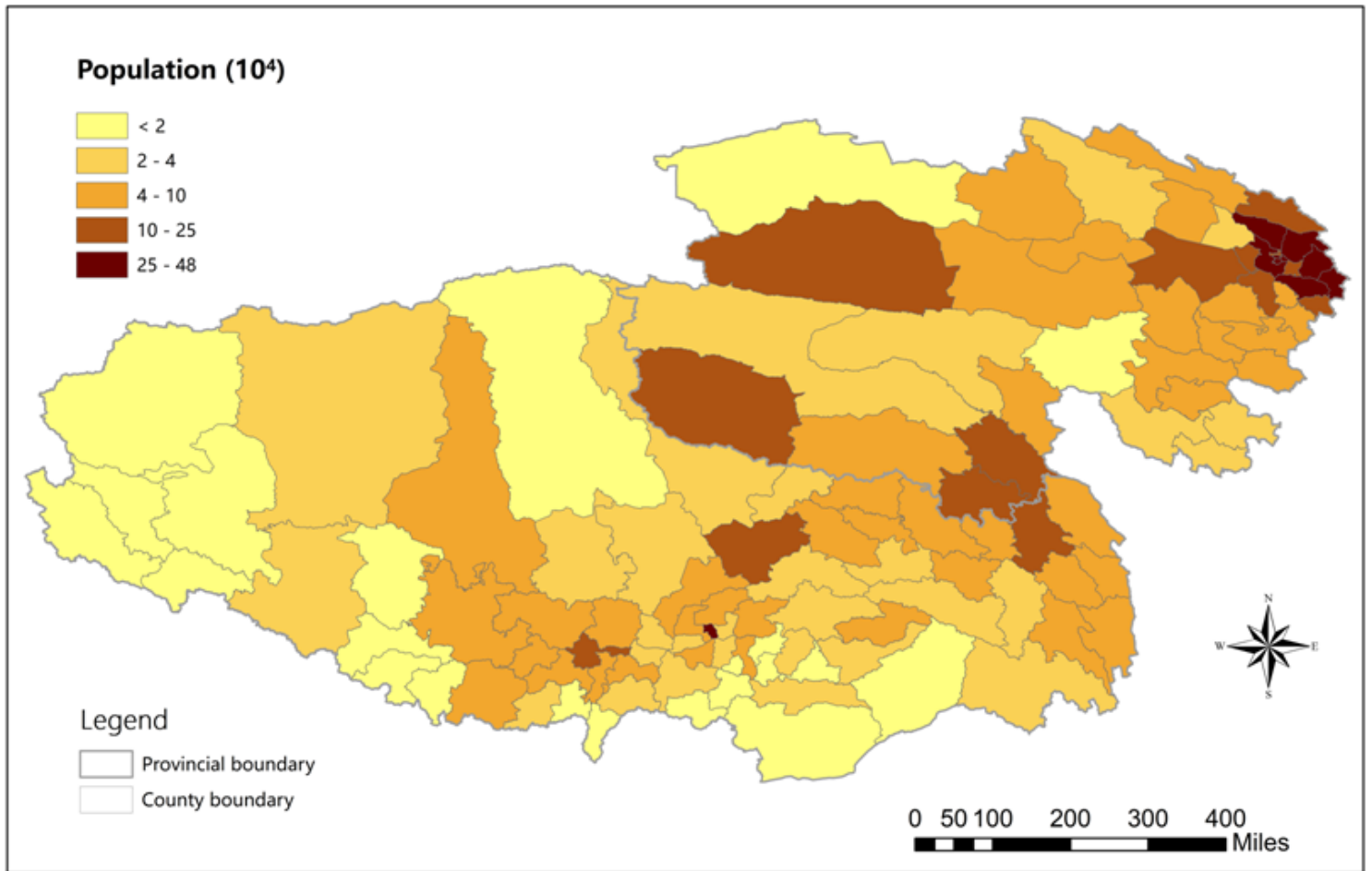


Figure 10

Population in the Tibetan Plateau by county.

Supplementary Files

This is a list of supplementary files associated with this preprint. Click to download.

- [Supplementary.docx](#)